Trajectory Approximation for Low-Performance Electric Sail with Constant Thrust Angle

Alessandro A. Quarta* and Giovanni Mengali†

University of Pisa, I-56122 Pisa, Italy

Nomenclature

$\boldsymbol{a}_p$	=	propulsive acceleration
a_c	=	characteristic acceleration
e	=	eccentricity
$\mathcal{E}$	=	specific mechanical energy
F	=	auxiliary function, see Eq. (11)
h	=	orbital angular momentum
$\hat{\boldsymbol{i}}_r$	=	radial unit vector
$\hat{\boldsymbol{i}}_\theta$	=	circumferential unit vector
O	=	Sun's center of mass
r	=	Sun-spacecraft distance ($r_\oplus \triangleq 1\,\text{AU}$)
t	=	time
$\mathcal{T}$	=	heliocentric polar reference frame
α	=	sail pitch angle
θ	=	polar angle
$\mu_\odot$	=	Sun's gravitational parameter
ρ	=	relative error in radial distance
χ	=	auxiliary variable, see Eq. (7)

Subscripts

0	=	initial, parking orbit

*Research Assistant, Department of Aerospace Engineering, a.quarta@ing.unipi.it. Senior Member AIAA.

†Associate Professor, Department of Aerospace Engineering, g.mengali@ing.unipi.it. Senior Member AIAA.

max = maximum

Superscripts

$\cdot$ = time derivative
$\star$ = critical
$\sim$ = numerical

Introduction

Analytic trajectories for a spacecraft subjected to a low, continuous, propulsive acceleration are available only for very special cases [1–3], even though these solutions find significant utility in preliminary mission design and optimization [4]. If a closed-form trajectory corresponding to a given thrust control law cannot be recovered, a possible option is to resort to a shape-based approach [5–7], or to suitably simplify the differential equations of motion [8–10].

Within the latter context, in this Note an analytical, albeit approximate, expression for the heliocentric trajectory of a spacecraft propelled by a low-performance electric sail [11, 12] is discussed. Using a two-dimensional model and under the assumptions of constant thrust angle and low propulsive acceleration modulus, the spacecraft heliocentric trajectory is obtained in a parametric way as a function of time. The effectiveness of the mathematical model is checked by comparing the analytic solution with a numeric integration of equations of motion.

Trajectory Approximation

Consider a spacecraft, whose propulsion system is an electric sail with characteristic acceleration a_c, that initially tracks a heliocentric (Keplerian) parking orbit. In analogy with the performance metrics used for solar sails [13], the spacecraft characteristic acceleration is defined as the maximum propulsive acceleration at a solar distance equal to one Astronomical

Unit. However, even though a solar sail and an electric sail are both capable of producing a propulsive thrust without the need of any propellant, these two propulsion systems are substantially different in terms of performance, shape, and dimensions [14].

Consider a two-dimensional scenario, and introduce a heliocentric polar reference frame $\mathcal{T}(O; r, \theta)$, where r is the Sun-spacecraft distance (with $r_\oplus \triangleq 1\,\text{AU}$) and θ is the polar angle measured counterclockwise from the Sun-spacecraft direction at the initial time instant $t_0 \triangleq 0$. According to recent numerical simulations [14], the electric sail thrust modulus varies inversely proportional to the Sun-spacecraft distance r. Therefore, the spacecraft propulsive acceleration vector $\boldsymbol{a}_p$ can be written as

$$\boldsymbol{a}_p = a_c \, \frac{r_\oplus}{r} \left(\hat{\boldsymbol{\imath}}_r \, \cos\alpha + \hat{\boldsymbol{\imath}}_\theta \, \sin\alpha \right) \tag{1}$$

where $\hat{\boldsymbol{\imath}}_r$ and $\hat{\boldsymbol{\imath}}_\theta$ are, respectively, the radial and circumferential unit vectors of $\mathcal{T}$, and $\alpha \in [-\alpha_{\max}, \alpha_{\max}]$ is referred to as sail pitch angle, with $\alpha_{\max} = 30\,\text{deg}$ [14]. Note that, in this simplified mission scenario, the pitch angle is the only system control parameter. If the propulsion system is switched-on at $t = t_0$, the spacecraft motion is described by the equations

$$\dot{\theta} = \frac{h}{r^2} \tag{2}$$

$$\ddot{r} = -\frac{\mu_\odot}{r^2} + \frac{h^2}{r^3} + \frac{a_c \, r_\oplus \, \cos\alpha}{r} \tag{3}$$

$$\dot{h} = a_c \, r_\oplus \, \sin\alpha \tag{4}$$

where h is the modulus of the osculating orbit's angular momentum vector, and $\mu_\odot$ is the Sun's gravitational parameter.

Assuming that the sail pitch angle α is maintained constant along the whole heliocentric

trajectory, Eq. (4) states that the angular momentum increases linearly with time according to the relationship

$$h = h_0 + (a_c\, r_\oplus \sin\alpha)\, t \tag{5}$$

where h_0 is the angular momentum along the heliocentric parking orbit. Note that Eq. (5) holds regardless of the parking orbit's eccentricity or the value of the characteristic acceleration. A constant pitch angle essentially corresponds to a constant angle between the electric sail nominal plane (that is, the mean plane containing the spacecraft charged tethers [15]) and the incoming solar wind flux. Such a simple control strategy is useful, for instance, for simplifying the design of both the spacecraft thermal and electrical power subsystems [14] .

Equation (5) provides a first integral of the motion, which can be substituted into Eq. (3) to facilitate the heliocentric trajectory analysis. In general, however, even with the aid of Eq. (5) an exact closed-form solution for the radial component of velocity $\dot{r}$ cannot be recovered. The only, notable, exception is obtained when $\alpha = 0$, that is, for a purely radial propulsive acceleration ($\boldsymbol{a}_p \cdot \hat{\boldsymbol{i}}_\theta = 0$). In that case h is constant along the whole trajectory, and Eq. (3) becomes an autonomous second-order differential equation in the variable r. A mission analysis for an electric sail subjected to a pure radial thrust is thoroughly discussed in Ref. [16] using the potential well concept by Prussing and Coverstone [17].

On the other hand, an approximate analytical expression for the spacecraft trajectory can be found if the initial parking orbit is circular (with radius $r_0 \triangleq h_0^2/\mu_\odot$) and the maximum modulus of the reference propulsive acceleration is sufficiently small. This scenario is consistent, for instance, with a low-performance electric sail (that is, a propulsion system of the first generation) that leaves the Earth's sphere of influence with zero hyperbolic excess velocity. Numerical simulations of a ten years flight time show that the time-variation of the dimensionless spacecraft radial acceleration $\ddot{r}/(\mu_\odot/r_0^2)$ fluctuates around a mean value on the order of 10^{-4} when $r_0 = r_\oplus$ and $a_c \leq 0.1\,\mathrm{mm/s^2}$.

This behaviour suggests the introduction of the approximation $\ddot{r} \approx 0$ into Eq. (3), in analogy with the classical work of Tsu [18, 19] about the logarithmic spiral solution for a solar sail spacecraft [20], or the Battin's method [10] for the spacecraft motion analysis under a circumferential, small, propulsive acceleration of constant modulus . The validity and the practical implications of such an assumption will be discussed afterwards with the aid of numerical simulations. For now, it suffices to observe that, as long as the left hand side of Eq. (3) is about zero, the right hand side of the same equation can be solved for r to get the Sun-spacecraft distance as a function of h, viz.

$$r = \frac{\mu_\odot}{2\, a_c\, r_\oplus\, \cos\alpha} \left(1 - \sqrt{1 - \frac{4\, a_c\, r_\oplus\, h^2\, \cos\alpha}{\mu_\odot^2}} \right) \tag{6}$$

Note that if $\alpha > 0$ (or $\alpha < 0$) the angular momentum h increases (or decreases) with time according to Eq. (5), and Eq. (6) implies an orbit raising (or lowering). In the limit as $a_c \to 0$, Eq. (6), when combined with Eq. (5), provides the exact value of the initial parking orbit's radius, that is, $r_0 = h_0^2/\mu_\odot$. If, instead, a_c is not zero but is sufficiently small, Eq. (6) gives a value of r slightly greater than r_0 and, therefore, does not meet exactly the initial boundary condition. The spacecraft trajectory can be obtained using a change of variable

$$\chi \triangleq 1 - \frac{4\, a_c\, r_\oplus\, h^2\, \cos\alpha}{\mu_\odot^2} \tag{7}$$

In fact, Eq. (6) is now rewritten as

$$r = \frac{\mu_\odot}{2\, a_c\, r_\oplus\, \cos\alpha} \left(1 - \sqrt{\chi} \right) \tag{8}$$

while Eq. (2) is turned into a differential equation with separable variables:

$$\frac{\mathrm{d}\theta}{\mathrm{d}\chi} = -\frac{\cot\alpha}{2\,\left(1-\sqrt{\chi}\right)^2} \tag{9}$$

which, under the assumption of $\alpha \neq 0$, can be integrated to yield the polar angle

$$\theta = \frac{F(\chi_0) - F(\chi)}{2\,\tan\alpha} \tag{10}$$

with

$$F(\chi) \triangleq \frac{2\left(1+\sqrt{\chi}\right)}{1-\chi} + \ln\left[\frac{(1-\chi)\,\left(1-\sqrt{\chi}\right)}{1+\sqrt{\chi}}\right] \tag{11}$$

where χ is given by Eq. (7) as a function of h, and $\chi_0 \triangleq \chi(h_0)$. Equations (8) and (10) are in the form $r = r(\chi)$ and $\theta = \theta(\chi)$ and, as such, they define the spacecraft heliocentric trajectory in a parametric form.

Moreover, the expression $r = r(\chi)$ can be used for evaluating the osculating orbit characteristics. In fact, bearing in mind Eqs. (5)-(6), a closed form approximation of the osculating orbit mechanical energy $\mathcal{E}$ is obtained as

$$\mathcal{E} = \frac{2\,h^2\,a_c^2\,r_\oplus^2\,\sin^2\alpha}{\mu_\odot^2 - 4\,a_c\,r_\oplus\,h^2\,\cos\alpha} + \frac{h^2}{2\,r^2} - \frac{\mu_\odot}{r} \tag{12}$$

Therefore, the semimajor axis and eccentricity of the osculating orbit are $a = -\mu_\odot/(2\,\mathcal{E})$ and $e = \sqrt{1 - 2\,\mathcal{E}\,h^2/\mu_\odot^2}$, where $\mathcal{E}$ is given by Eq. (12) as a function of h. As before, if $a_c \to 0$, Eq. (12) is exact ($\mathcal{E} = -0.5\,\mu_\odot/r_0$), while if a_c is small, but not zero, the corresponding initial value of $\mathcal{E}$ is slightly overestimated.

The intrinsic limit of the previous mathematical model is in the form of Eq. (6). In fact,

if $\alpha > 0$, the term under the square root in Eq. (6) will become negative when $t > t^\star$, where

$$t^\star = \frac{\mu_\odot/(2\sqrt{a_c\, r_\oplus\, \cos\alpha}) - h_0}{a_c\, r_\oplus\, \sin\alpha} \qquad \text{with} \qquad \alpha \in (0,\, \alpha_{\max}] \tag{13}$$

Anyway, the preceding equation shows that $t^\star$ is a decreasing function of both a_c and α. In particular, recalling that the current electric sail design [15] requires that $\alpha \leq 30\,\text{deg}$, and assuming $r_0 = r_\oplus$ (that is, $h_0 = \sqrt{\mu_\odot\, r_\oplus} = 2\,\pi\,\text{AU}^2/\text{year}$) and $a_c \leq 0.1\,\text{mm/s}^2$, Eq. (13) provides $t^\star \geq 59.2\,\text{years}$, a value greater than any flight time of practical interest.

Numerical Simulations

The accuracy of the previous analytical results can be compared, by simulation, with a numerical integration of equations of motion (2)–(4) using, in both cases, the same parking orbit radius, and the same propulsion system characteristics, that is, a_c and α. The numerical integrations have been performed through a variable order Adams-Bashforth-Moulton solver [21] with absolute and relative errors of 10^{-12}.

Assuming $r_0 = r_\oplus$, $a_c = 0.1\,\text{mm/s}^2$ and $\alpha = \alpha_{\max}$, the comparison is summarized in Fig. 1 for a ten-years time interval. Figure 1 clearly shows that the analytical approximations of $\mathcal{E}$ and of θ closely follow their numerical counterparts.

On the contrary, the numerical simulations of radial distance and eccentricity exhibit an oscillatory behavior superimposed to a secular variation, which is essentially described by Eq. (6). This is confirmed by Fig. 2 in which the time histories of radial ($\dot{r}$) and circumferential (h/r) velocities have been normalized through the circular velocity along the parking orbit ($\sqrt{\mu_\odot/r_\oplus}$). Note that the analytical expressions of both velocity components do not satisfy the actual initial conditions, but fit well their mean values.

On the other hand, the spacecraft trajectory obtained using Eqs. (8) and (10) closely follows the trajectory calculated numerically, as is shown in Fig. 3. The difference between the

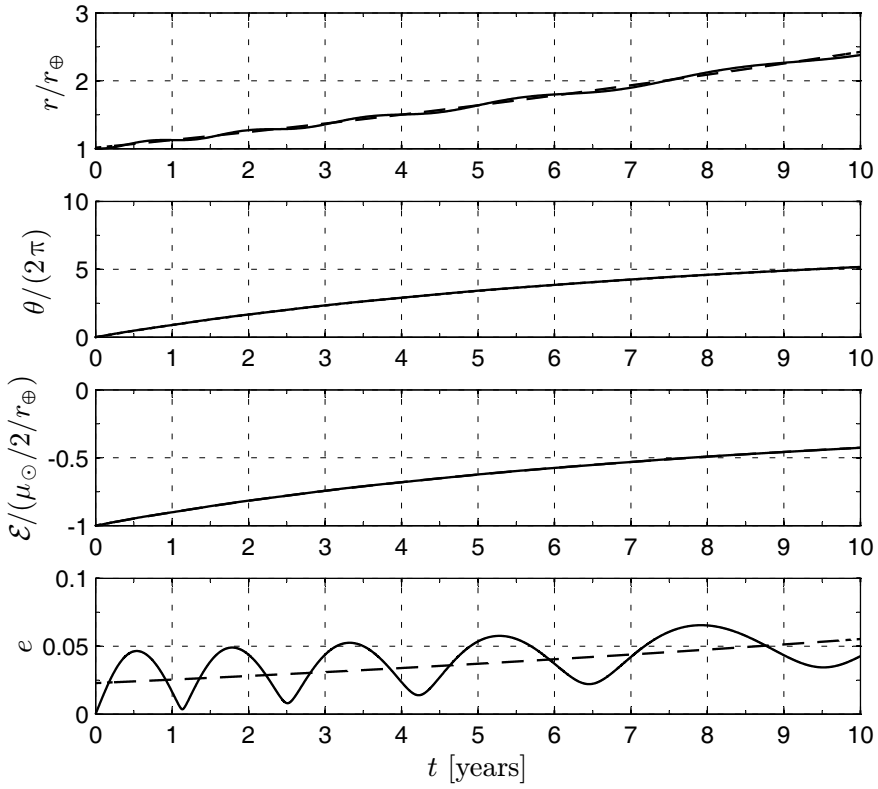

Figure 1: **Simulation results for a ten-years orbit raising with $a_c = 0.1\,\mathrm{mm/s^2}$, $\alpha = 30\,\mathrm{deg}$, and $r_0 = r_\oplus$ (solid line = numerical; dashed line = analytical).**

two trajectories is better appreciated in terms of relative error in radial distance $\rho \triangleq |\widetilde{r}(\theta) - r(\theta)|/\widetilde{r}(\theta)$ for a given value of polar angle θ, where $\widetilde{r}(\theta)$ is the actual Sun-spacecraft distance evaluated through numerical integration . Figure 4 shows the maximum (relative) distance error ρ, over a ten-years simulation, as a function of $a_c \in [0.01, 0.1]\,\mathrm{mm/s^2}$ and the sail pitch angle $\alpha = \pm\{30, 20, 10, 1\}\,\mathrm{deg}$. For a given value of a_c, the maximum error increases linearly with $|\alpha|$, for both an orbit raising (Fig. 4(a)) and an orbit lowering (Fig. 4(b)). Notably, the difference between the approximated trajectory and the numerical solution is always moderate, and the maximum value of ρ is of a few percent only, even for long time intervals.

The previous analytical relationships are useful to obtain an estimate of the flight time required by an electric sail to reach a prescribed distance from the Sun. For example, in

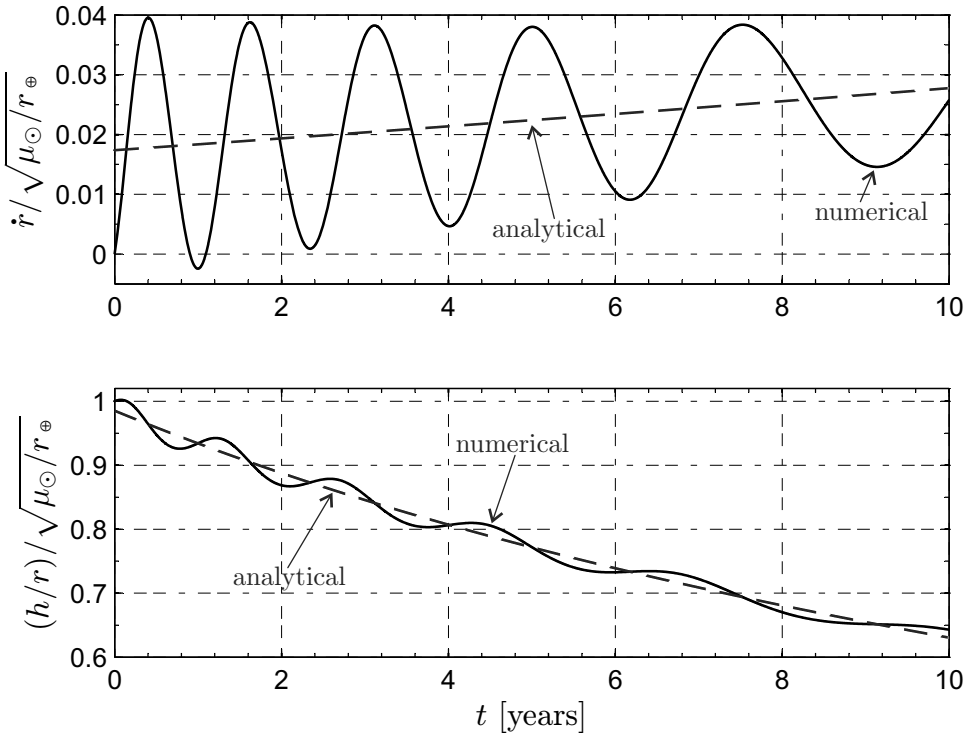

Figure 2: **Components of spacecraft velocity** ($a_c = 0.1\,\mathrm{mm/s^2}$, $\alpha = 30\,\mathrm{deg}$, **and** $r_0 = r_\oplus$).

a hypothetical flyby mission toward Mars ($r = 1.524\,\mathrm{AU}$), assuming $a_c = 0.1\,\mathrm{mm/s^2}$ and $\alpha = 30\,\mathrm{deg}$, the flight time obtained integrating the equations of motion is 1603 days, while Eqs. (5)-(6) provide a flight time of 1521 days, with a percentage difference of 5% only with respect to the value obtained by simulation. This difference is further reduced in a flyby mission to Venus ($r = 0.723\,\mathrm{AU}$, $a_c = 0.1\,\mathrm{mm/s^2}$ and $\alpha = -30\,\mathrm{deg}$) in which the mission time is 1061 days (numerical simulation), while the analytic model estimates 1063 days.

Another potential application, not directly related to the trajectory approximation, concerns a minimum time rendez-vous problem between two circular and coplanar orbits. In this case it is possible to obtain a precise information about the time interval along which the propulsion system is switched-on. In fact, although the optimal control law allows a variation of the sail pitch angle between their extremal values [22], numerical simulations of a low-performance electric sail show that $\alpha = \alpha_{\max}$ in an optimal orbit raising, or $\alpha = -\alpha_{\max}$

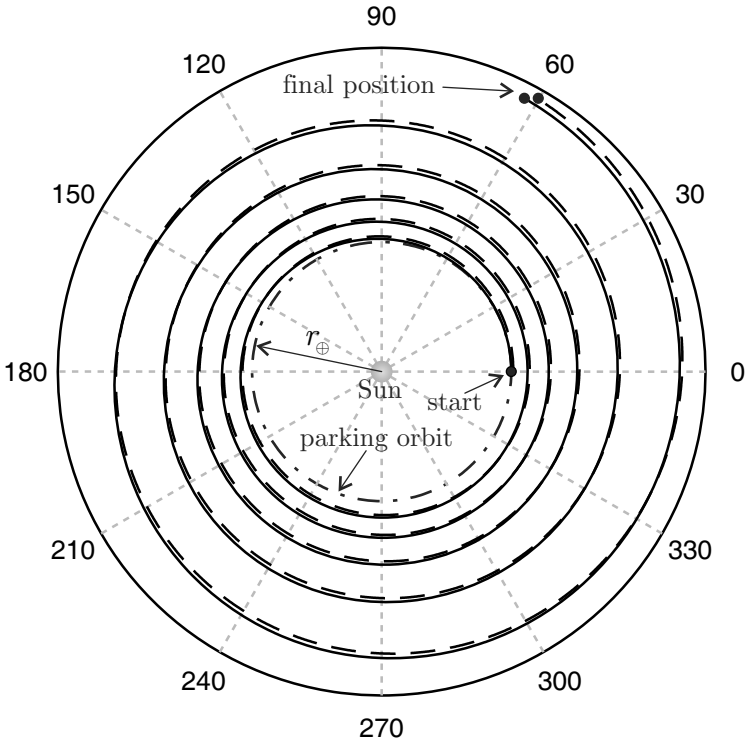

Figure 3: **Spacecraft trajectory in a ten years orbit raising ($a_c = 0.1\,\mathrm{mm/s^2}$, $\alpha = 30\,\mathrm{deg}$, and $r_0 = r_\oplus$).**

in an optimal orbit lowering. In other terms, the spacecraft optimal trajectory consists of a sequence of propelled or coasting arcs in which $|\alpha|$ is equal to its maximum value. As a result, the thrusting time is obtained from Eq. (5) by setting h equal to the target orbit's angular momentum modulus and solving for t. For example, a minimum time (simplified) Earth-Mars transfer with $a_c = 0.1\,\mathrm{mm/s^2}$ requires a flight time of 1782 days, with a thrusting time of 1617 days. The latter coincides with the value obtained from Eq. (5) when $h = \sqrt{\mu_\odot\, r}$, with $r = 1.524\,\mathrm{AU}$.

Conclusions

This Note has discussed an analytical, approximated, model for calculating the heliocentric trajectory of a low-performance electric sail. Under the assumption of constant sail pitch angle, the spacecraft trajectory can be found in a parametric way and the main char-

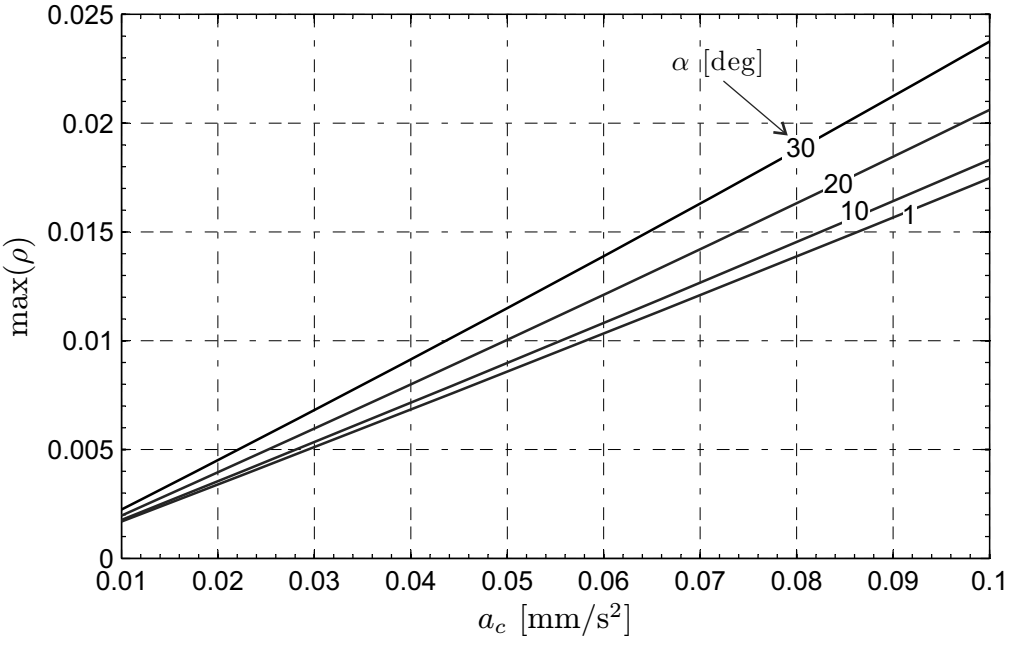

a) orbit raising ($\alpha > 0$).

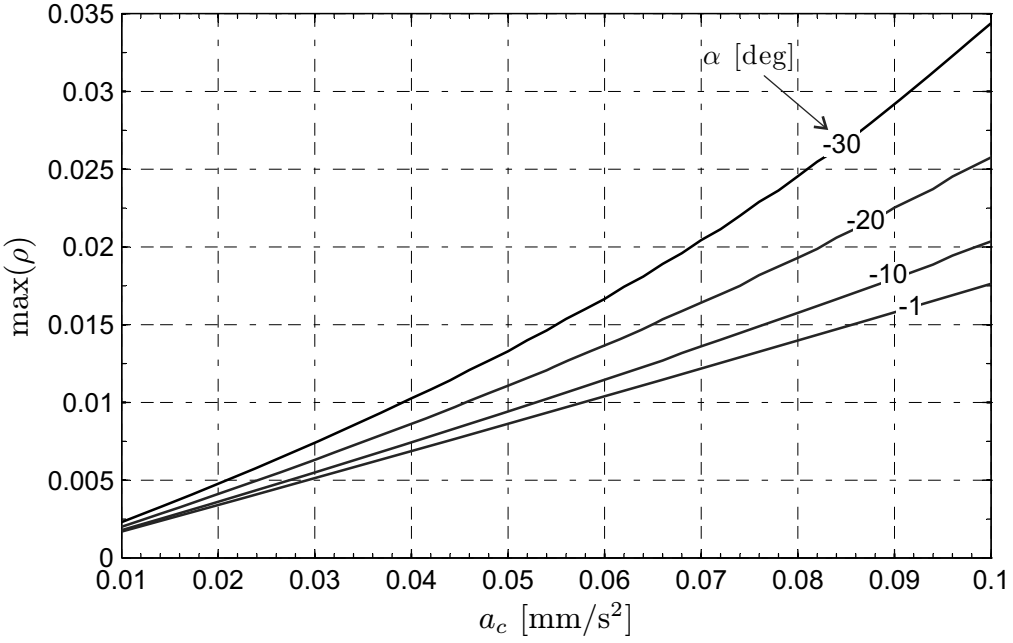

b) orbit lowering ($\alpha < 0$).

Figure 4: Maximum (relative) error in radial distance, for a ten-years mission as a function of the characteristic acceleration ($r_0 = r_\oplus$).

acteristics of the osculating orbit can be obtained as a function of the flight time. The numerical simulations confirm the accuracy of the analytical solution even on timescales of several years.

Acknowledgments

This research was financed within the European Community's Seventh Framework Programme ([FP7/2007-2013]) under grant agreement number 262733.

References

[1] Markopoulos, N., "Analytically exact non-Keplerian motion for orbital transfers," *AIAA/AAS Astrodynamics Conference*, Scottsdale, AZ, August, 1–3 1994, Paper AIAA-1994-3758.

[2] Petropoulos, A. E. and Sims, J. A., "A review of some exact solutions to the planar equations of motion of a thrusting spacecraft," *2nd International Symposium on Low-Thrust Trajectory (LoTus-2)*, Toulouse, France, June, 18–20 2002.

[3] McInnes, C. R., "Orbits in a Generalized Two-Body Problem," *Journal of Guidance, Control, and Dynamics*, Vol. 26, No. 5, September–October 2003, pp. 743–749. doi: 10.2514/2.5129.

[4] Izzo, D., "Lambert's Problem for Exponential Sinusoids," *Journal of Guidance, Control, and Dynamics*, Vol. 29, No. 5, September-October 2006, pp. 1242–1245. doi: 10.2514/1.21796.

[5] Petropoulos, A. and Longuski, J., "Shape-Based Algorithm for the Automated Design of Low-Thrust, Gravity Assist Trajectories," *Journal of Spacecraft and Rockets*, Vol. 41, No. 5, September-October 2004, pp. 787–796. doi: 10.2514/1.13095.

[6] Wall, B. and Conway, B., "Shape-Based Approach to Low-Thrust Rendezvous Trajectory Design," *Journal of Guidance, Control and Dynamics*, Vol. 32, No. 1, January-February 2009, pp. 95–101. doi: 10.2514/1.36848.

[7] Novak, D. and Vasile, M., "Improved Shaping approach to the preliminary design of low-thrust trajectories," *Journal of Guidance, Control and Dynamics*, Vol. 34, No. 1, January-February 2011, pp. 128–147. doi: 10.2514/1.50434.

[8] Wiesel, E. E. and Alfano, S., "Optimal Many-Revolution Orbit Transfer," *Journal of Guidance, Control, and Dynamics*, Vol. 8, No. 1, January-February 1985, pp. 155–157. doi: 10.2514/3.19952.

[9] Alfano, S. and Thorne, J. D., "Circle-to-Circle Constant-Thrust Orbit Raising," *Journal of the Astronautical Sciences*, Vol. 42, No. 1, January–March 1994, pp. 35–45.

[10] Battin, R. H., *An Introduction to the Mathematics and Methods of Astrodynamics*, AIAA Education Series, AIAA, New York, 1987, p. 418, ISBN: 1-563-47342-9.

[11] Janhunen, P., "Electric Sail for Spacecraft Propulsion," *Journal of Propulsion and Power*, Vol. 20, No. 4, July-August 2004, pp. 763–764. doi: 10.2514/1.8580.

[12] Janhunen, P. and Sandroos, A., "Simulation Study of Solar Wind Push on a Charged Wire: Basis of Solar Wind Electric Sail Propulsion," *Annales Geophysicae*, Vol. 25, No. 3, 2007, pp. 755–767. doi: 10.5194/angeo-25-755-2007.

[13] McInnes, C. R., *Solar Sailing: Technology, Dynamics and Mission Applications*, Springer-Praxis Series in Space Science and Technology, Springer-Verlag, Berlin, 1999, pp. 13–14.

[14] Janhunen, P. et al., "Electric solar wind sail: Towards test missions," *Review of Scientific Instruments*, Vol. 81, No. 11, November 2010, pp. 111301–1–111301–11. doi: 10.1063/1.3514548.

[15] Janhunen, P., "Status report of the electric sail in 2009," *Acta Astronautica*, Vol. 68, No. 5–6, March-April 2011, pp. 567–570. doi: 10.1016/j.actaastro.2010.02.007.

[16] Mengali, G., Quarta, A. A., and Aliasi, G., "A Graphical Approach to Electric

Sail Mission Design with Radial Thrust," *Acta Astronautica*, 2012 (in press). doi: 10.1016/j.actaastro.2012.03.022.

[17] Prussing, J. E. and Coverstone, V. L., "Constant Radial Thrust Acceleration Redux," *Journal of Guidance, Control, and Dynamics*, Vol. 21, No. 3, May-June 1998, pp. 516–518. doi: 10.2514/2.7609.

[18] Tsu, T. C., "Interplanetary Travel by Solar Sail," *American Rocket Society Journal*, Vol. 29, No. 6, June 1959, pp. 422–427.

[19] London, H. S., "Some Exact Solutions of the Equations of Motion of a Solar Sail With a Constant Setting," *American Rocket Society Journal*, Vol. 30, No. 2, February 1960, pp. 198–200.

[20] Bacon, R. H., "Logarithmic Spiral: An Ideal Trajectory for the Interplanetary Vehicle with Engines of Low Sustained Thrust," *American Journal of Physics*, Vol. 27, No. 3, March 1959, pp. 164–165. doi: 10.1119/1.1934788.

[21] Shampine, L. F. and Reichelt, M. W., "The MATLAB ODE Suite," *SIAM Journal on Scientific Computing*, Vol. 18, No. 1, January 1997, pp. 1–22. doi: 10.1137/S1064827594276424.

[22] Mengali, G., Quarta, A. A., and Janhunen, P., "Electric Sail Performance Analysis," *Journal of Spacecraft and Rockets*, Vol. 45, No. 1, January–February 2008, pp. 122–129. doi: 10.2514/1.31769.